

# Piecemeal Quantum Telescope with Super Efficiency

Jian Leng,<sup>1</sup> Yi-Xin Shen,<sup>1</sup> Zhou-Kai Cao,<sup>1</sup> and Xiang-Bin Wang<sup>1, 2, 3, 4, \*</sup>

<sup>1</sup>*State Key Laboratory of Low Dimensional Quantum Physics, Department of Physics, Tsinghua University, Beijing 100084, China*

<sup>2</sup>*Jinan Institute of Quantum Technology and Jinan branch, Hefei National Laboratory, Jinan, Shandong 250101, China*

<sup>3</sup>*International Quantum Academy, Shenzhen 518048, China*

<sup>4</sup>*Frontier Science Center for Quantum Information, Beijing 100193, China*

Detecting remote objects with higher precision takes a crucial role in many scientific tasks, such as astronomical observation. The precision of existing quantum telescopes is improved in the scale of square root of incident single-photons. Here we propose the piecemeal quantum telescope with high efficiency through bit-by-bit iteration. It improves precision exponentially requesting only a small number of incident single-photons in detecting the star angle. As a result, it requests to detect only a few hundreds of photons for a precision breaking classical limit by 4 to 5 magnitude orders. Moreover, our method can be applied to distinguish a general astronomical target consisting of unknown number of stars with high resolution.

## I. INTRODUCTION

Quantum imaging can detect more information than classical imaging by applying quantum interferometry [1–11]. Especially, quantum telescopes [1–4] can detect more precise angle value of single-star target than classical telescope. The light from a remote source is attenuated to single-photon level when arriving at ground. Therefore it is meaningful to investigate efficient method which can detect the angle value precisely with a small number of incident single-photons. The precision of existing quantum telescopes is improved in the scale of square root of incident single photons. Here we propose the piecemeal quantum telescope whose precision in detecting remote star target is exponentially improved with number of incident single photons detected. Our method works in the way of bit-by-bit iteration, reaching a high precision breaking the classical limit by several magnitude orders while requesting to detect only a few hundreds of single-photons. Therefore it is useful in the practical case with very weak incident light from the remote target. Our method can also be applied to distinguish the general astronomical target with unknown number of stars with high resolution.

## II. SINGLE-STAR ASTRONOMICAL TARGET

The proposed set-up of our piecemeal quantum telescope is schematically shown in Fig. 1. There are  $K+1$  pairs of receivers and we collect data from each pair of them. For any pair of receivers denoted by  $k$ , the distance between those two receivers (baseline) is  $L_k$ , where  $k = \{0, 1, \dots, K\}$ . Suppose that the astronomical target is a single star with a small angle  $\theta$  as shown in Fig. 1(a). The state single photon arriving at two receivers of pair

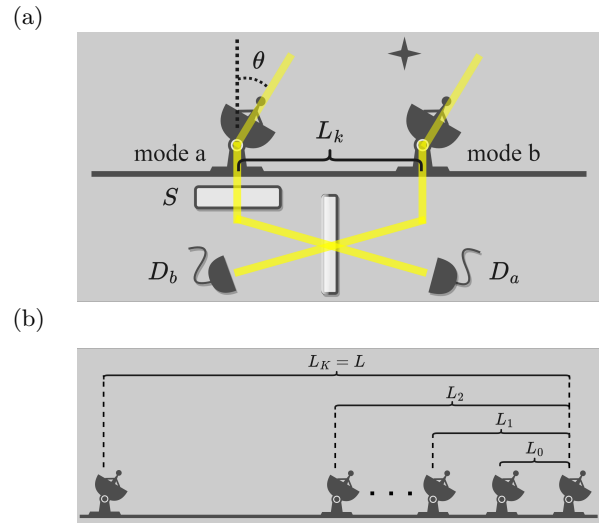


FIG. 1. (a) Collecting data from a pair of receivers with phase shifter  $S$ , 50:50 beam splitter, threshold detectors  $D_a$  and  $D_b$ . (b) Our piecemeal quantum telescope for a single star. In each iteration, it collects data from a pair of receivers with distance  $L_k$ . The maximal distance is  $L$ .

$k$  is

$$|\Psi_k\rangle = \frac{1}{\sqrt{2}}(|01\rangle + e^{i\phi_k}|10\rangle), \quad \phi_k \approx 2\pi \frac{L_k}{\lambda} \theta. \quad (1)$$

Here  $\lambda$  is the wavelength,  $|c_a c_b\rangle$  represents photon numbers of mode  $a$  and  $b$  and  $\phi_0 \in [0, 2\pi)$ . We set zero and  $\frac{\pi}{2}$  phase shifts of  $S$  to collect the first and second set of data, respectively. We set  $L_k = (\frac{1}{2})^k L_0$  at this moment and derive our calculation formula Eq. (3) with this setting. Latter, through similar derivation, we shall present the calculation formula in Eq. (12) with more general mathematical setting of baseline length  $L_{k+1} = s_k L_k$  latter.

We start with some mathematical notations.

1) Taking  $L_k = 2^k L_0$  and hence  $\phi_{k+1} = 2\phi_k$ .

2)  $\dot{x} = x \bmod 2\pi$ . When using  $\alpha \cdot \dot{x}$ , we mean  $\alpha \cdot (x \bmod 2\pi)$ .  
 3)  $\hat{\phi}_k$ : The observed value of  $\dot{\phi}_k$ . In our setup  $\hat{\phi}_k$  is obtained based on the experimentally collected data. Details are shown around Eq. (4) in Sec. III.

In our calculation below we introduce a new variable

$$\psi_k = \phi_k - \hat{\phi}_k + \pi,$$

and its modulo

$$\dot{\psi}_k = (\phi_k - \hat{\phi}_k + \pi) \bmod 2\pi.$$

The definition of  $\psi_k$  means  $\psi_{k+1} = \phi_{k+1} - \hat{\phi}_{k+1} + \pi$ . As shown in the Sec. I of Supplementary Material [12], the following equation

$$2 \cdot \dot{\psi}_k = \dot{\psi}_{k+1} + \dot{r}_{k+1} \quad (2)$$

can hold with a small failure probability if the observation error is not too large. Here  $r_{k+1} = \hat{\phi}_{k+1} - 2\hat{\phi}_k + \pi$ . Using Eq. (2) iteratively we obtain

$$\dot{\psi}_0 = \sum_{k=1}^K \left(\frac{1}{2}\right)^k \dot{r}_k + \left(\frac{1}{2}\right)^K \dot{\psi}_K.$$

Recalling the definition  $\dot{\psi}_0 = (\phi_0 - \hat{\phi}_0 + \pi) \bmod 2\pi$  and taking the approximation  $\dot{\psi}_K = \pi$ , we obtain

$$\phi_0 = \left( \hat{\phi}_0 - \pi + \sum_{k=1}^K \left(\frac{1}{2}\right)^k \dot{r}_k + \left(\frac{1}{2}\right)^K \pi \right) \bmod 2\pi. \quad (3)$$

Here we have used  $\phi_0 = \dot{\phi}_0$ , as we requested  $\phi_0 \in [0, 2\pi)$  earlier. This is the major formula of this letter. Since  $(\frac{1}{2})^k$  represents  $k$ th binary bit after the decimal point, we see a bit-by-bit iteration behavior in the term  $\sum_{k=1}^K \left(\frac{1}{2}\right)^k \dot{r}_k$  with the summation direction  $k$  from  $K$  to 1. Numerical simulation below indeed gives satisfactory results with Eq. (3).

### III. PERFORMANCE FOR SINGLE-STAR ASTRONOMICAL TARGET

To do calculation by Eq. (3), we need the observed values  $\{\hat{\phi}_k | k = 0, 1, \dots, K\}$  as the input. In our calculation, we can produce these values based on experimental data. In our proposed set-up Fig. 1, we shall collect two sets of data. The first (second) set is obtained through setting zero ( $\frac{\pi}{2}$ ) phase shift on  $S$ . In the first (second) set, we observe the event of detector  $D_a$  silent and  $D_b$  clicking for  $m_k$  ( $\bar{m}_k$ ) times in total detected events of one-detector-clicking  $M_k$  ( $\bar{M}_k$ ). We have

$$\hat{\phi}_k = \frac{1}{2} \left( \cos^{-1} q_k + \sin^{-1} \bar{q}_k \right) \bmod 2\pi, \quad (4)$$

where

$$q_k = 1 - \frac{2m_k}{M_k}, \quad \bar{q}_k = \frac{2\bar{m}_k}{\bar{M}_k} - 1. \quad (5)$$

In this work, we shall only consider the important practical issue of small data size with possible statistical errors but we assume perfect devices. For imperfect devices, see Section II of Supplementary Material [12].

Since  $M_k$  and  $\bar{M}_k$  are finite number in practical detection, the  $\phi_0$  value calculated by Eq. (3) does not exactly equal to the actual value of  $\phi_0$ . Denoting  $\tilde{\phi}_0$  as the  $\phi_0$  value calculated by Eq. (3), we define the failure probability  $\epsilon$  as

$$\epsilon = P(|\tilde{\phi}_0 - \phi_0| > \frac{\pi}{2^{K+1}}).$$

This gives the precision of our piecemeal method

$$\delta\phi = \frac{\pi}{2^{K+1}}, \quad \delta\theta = \frac{\lambda}{2\pi L_0} \delta\phi = \frac{\lambda}{4L}. \quad (6)$$

In our numerical simulation, we first generate a set of ‘experimental data’  $\{m_k, \bar{m}_k\}$ , according to the probability distributions  $P(m_k | M_k)$  and  $P(\bar{m}_k | \bar{M}_k)$  given by known phase value  $\phi_0$ . They obey Binomial distributions

$$P(m_k | M_k) = C_{M_k}^{m_k} p_k^{m_k} (1 - p_k)^{M_k - m_k}, \\ P(\bar{m}_k | \bar{M}_k) = C_{\bar{M}_k}^{\bar{m}_k} \bar{p}_k^{\bar{m}_k} (1 - \bar{p}_k)^{\bar{M}_k - \bar{m}_k}, \quad (7)$$

where  $p_k = \frac{1}{2}(1 - \cos 2^k \phi_0)$  and  $\bar{p}_k = \frac{1}{2}(1 + \sin 2^k \phi_0)$ . Using  $\{m_k, \bar{m}_k\}$ , we calculate the estimated value  $\tilde{\phi}_0$  by Eq. (3). If  $|\phi_0 - \tilde{\phi}_0| < \delta\phi$ , we regard it as a successful event otherwise a failure event. Repeating it many times, we calculate the ratio of number of failure events and the total number of events which gives the failure probability  $\epsilon$ . We take simulations for many different  $\phi_0$  values from 0 to  $2\pi$ . To quantify the performance, all  $\{M_k, \bar{M}_k\}$  are taken as the same value  $M$  and we set  $K = 14$ . Numerical results for  $M = 1, 4$  and  $7$  are shown in Fig. (2). We take  $M = 7$  in following discussions.

If we use quantum memory with error correction [3], we do not have to consider photon loss in transmission from each receivers. Therefore the total number of single-photons at receives is  $M_t = 2M(K+1)$ . Applying Eq. (6), we have  $\delta\theta = \frac{\lambda}{2L_0} 2^{-\frac{M_t}{2M}} \propto 2^{-M_t}$ . Numerical simulation of the performance of our method is shown in Fig. 3(a), where we have taken comparison with classical telescope  $\delta\theta_c$  (Hubble Space Telescope, diameter  $D = 2.4\text{m}$ ) and existing quantum telescopes  $\delta\theta_Q$  [1–4]. In the calculation, we take  $M = 7$  and  $\lambda = 628\text{nm}$ . For a fair comparison, we assume the same initial crude information of angle range  $(0, \theta_{\max})$  for both the existing quantum telescopes and our method. We take  $\theta_{\max} = 10\text{mas}$  and obtain  $L_0 \approx \frac{\lambda}{\theta_{\max}} = 13\text{m}$  from Eq. (1). Calculation details for classical telescope and existing quantum telescopes

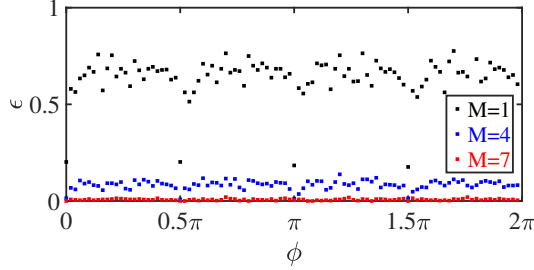


FIG. 2. The failure probability  $\epsilon$  changes with  $\phi$  for detecting single-star target. We take  $M_k = \bar{M}_k = M$  for every  $k$ . For the red data points in the figure, we assume the number of detected photons is  $2 \times 7 = 14$  for each baseline and the total number of detected photons is  $14(K+1) = 210$ , and the failure probability for this case is around 0.0073, less than 1%. Each data point is obtained by averaging 500 samples.

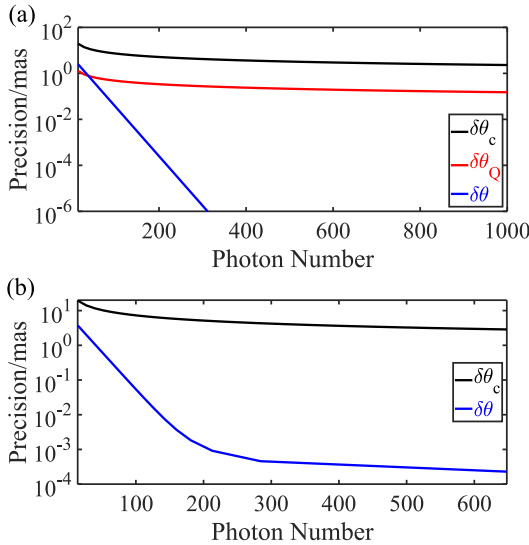


FIG. 3. Precisions of Hubble Space Telescope  $\delta\theta_c$ , existing quantum telescope  $\delta\theta_Q$  and our piecemeal quantum telescope  $\delta\theta$  for detecting single-star target. The horizontal axis is the total number  $M_t$  of incident single-photons to receivers. (a) Using quantum memory for  $\delta\theta_Q$  and  $\delta\theta$ . (b) Not using quantum memory. Our proposed piecemeal quantum telescope reaches the observation precision within the uncertainty of  $\theta = 10^{-3}$ mas requesting about 212 received photons (totally 182 detected photons in  $K+1 = 14$  baselines).

are shown in Section III in Supplementary Material [12].

Now we consider the performance without quantum memory. The channel transmittance is  $\eta(l)$  of optical fiber of length  $l$ . We need the baseline of length  $L_k = 2^k L_0$  for pair  $k$ . Suppose that beam splitter locates at the middle of fiber. The transmittance of optical fiber is  $\eta(2^{k-1}L_0)$ . The incident single-photons at receivers have a probability  $\eta(2^{k-1}L_0)$  to arrive at detectors. So the total number of collected single-photons at receivers is  $M_t = \sum_{k=0}^K \frac{2M}{\eta(2^{k-1}L_0)}$ . Applying Eq. (6), we can obtain a relation between precision and total

photon number  $\delta\theta(M_t)$ . We compare our result with Hubble Space Telescope  $\delta\theta_c$  in Fig. 3(b). We take standard optical fiber, that is  $\eta(l) = 10^{(-\alpha L/10)}$  where  $\alpha = 0.2$  and  $l_0 = 10\text{km}$ . We set  $M = 7$ ,  $\theta_{\max} = 15\text{mas}$  and obtain  $L_0 \approx \frac{\lambda}{\theta_{\max}} = 8.6\text{m}$  from Eq. (1). When  $\delta\theta \approx 10^{-3}\text{mas}$ , we have  $K = 13$  then the length of fiber is  $2^{K-1}L_0 \approx 35\text{km}$  that is feasible for practical application.

#### IV. APPLICATION TO GENERAL ASTRONOMICAL TARGET

Our piecemeal method can be applied to distinguish a general astronomical target that contains unknown number of stars. Compared with the existing result [8, 11] of recognizing binary stars, our result here can distinguish a single star or multiple-stars with unknown number of stars, not limited to binary stars. Suppose there are  $N$  stars in an astronomical target. The state of single photon arriving at two receivers from  $n$ th star is

$$|\Psi_k^{(n)}\rangle = \frac{1}{\sqrt{2}}(|01\rangle + e^{i\phi_k^{(n)}}|10\rangle), \quad \phi_k^{(n)} \approx 2\pi \frac{L_k}{\lambda} \theta^{(n)}, \quad (8)$$

where  $\theta^{(n)}$  is the angle of  $n$ th star and  $L_k = 2^k L_0$ . Suppose that the received single photon is emitted by  $n$ th star with probability  $p_n$ . Following the same procedure of detecting single-star target, we obtain the data  $\{q_k, \bar{q}_k | k = 0, 1, \dots, K\}$  in Eq. (5). We introduce functional

$$g_k(\omega) = \frac{1}{2} (1 - q_{k+1} \cos 2\omega + \bar{q}_{k+1} \sin 2\omega) - (q_k \sin \omega + \bar{q}_k \cos \omega)^2,$$

for  $k = \{0, 1, \dots, K-1\}$ . Maximizing  $g_k(\omega)$  we obtain

$$\max_{\omega} g_k(\omega) = g_k(\omega_k). \quad (9)$$

*Theorem 1:* Asymptotically, the sufficient and necessary condition for  $N = 1$  (single star) is that  $g_k(\omega_k) = 0$  for  $\forall k = \{0, 1, \dots, K-1\}$ .

The proof is shown in Section IV of Supplementary Material [12]. In practice, we cannot obtain  $g_k(\omega)$  with infinite accuracy. So we apply the following method:

*Method 1:* If  $g_k(\omega_k) \leq \bar{g}$  in every iteration, it is a single star; else it contains multiple stars. Here  $\bar{g}$  is a small positive value. As shown in our simulation,  $\bar{g}$  value and the number of detected photons are related to the failure probability. Below we study the resolution of Method 1. Consider two stars with  $\phi_0^{(1)}, \phi_0^{(2)}$  and  $p_1 = p_2 = 0.5$ . If  $\Delta\phi = \phi_0^{(2)} - \phi_0^{(1)} = \frac{\pi}{2^K}$ , we have  $g_{K-1}(\omega_{K-1}^0) = \frac{1}{2} > \bar{g}$  (remember  $\bar{g}$  is small). We successfully conclude that it is not a single star. So the resolution is better than

$$\Delta\theta = \frac{\lambda}{2\pi L_0} \Delta\phi = \frac{\lambda}{2L}. \quad (10)$$

In the numerical simulation, we first generate a set of ‘experimental data’  $\{m_k, \bar{m}_k\}$ , according to the probability distributions  $P(m_k|M_k)$  and  $P(\bar{m}_k|\bar{M}_k)$  given by known phase values  $\{\phi_0^{(n)}\}$ . The form of distributions is still given by Eq. (7), but the parameter  $p_k$  and  $\bar{p}_k$  change to

$$p_k = \frac{1}{2}(1 - \sum_{n=1}^N \cos 2^k \phi_0^{(n)}), \quad \bar{p}_k = \frac{1}{2}(1 + \sum_{n=1}^N \sin 2^k \phi_0^{(n)}).$$

Using  $\{m_k, \bar{m}_k\}$ , we obtain  $\{q_k, \bar{q}_k\}$  in Eq. (5) which is the input of Eq. (9). We numerically simulate the failure probabilities of following two cases.

1) The single-star target is wrongly recognized as multiple stars:

$$\epsilon_1(\phi_0) = \\ P(\text{Method 1 concludes multiple stars for a single star}).$$

2) The two-star target is wrongly recognized as a single star:

$$\epsilon_2(\phi_0^{(1)}, \phi_0^{(2)}) = \\ P(\text{Method 1 concludes a single star for two stars}).$$

We take all values in  $\{M_k, \bar{M}_k\}$  as the same value  $M$ ,  $\phi_0 \in (0, 2\pi)$ ,  $\phi_0^{(1)} = \pi$ ,  $\phi_0^{(2)} \in (0, \pi - \Delta\phi) \cup (\pi + \Delta\phi, 2\pi)$ ,  $p_1 = p_2 = 0.5$ ,  $\bar{g} = 0.1$  and  $K = 13$ . The simulation results for  $\epsilon_1$  with  $M = 10^2$ ,  $10^3$  and  $10^4$  are shown in Fig. 4(a). We take  $M = 10^4$  in following discussions. The simulation results for  $\epsilon_2$  with  $M = 10^4$  are shown in Fig. 4(b).

If we use quantum memory with error correction [3], we do not have to consider photon loss in transmission from each receivers in applying Eq. (10). Therefore  $\Delta\theta = \frac{\lambda}{L_0} 2^{\frac{-M_t}{2M}}$  where  $M_t$  is the total received single-photon number. For a classical telescope with diameter  $D$ , the resolution is given by Rayleigh limit  $\Delta\theta_c = \frac{1.22\lambda}{D}$  [13, 14]. We take  $M = 10^4$ ,  $\lambda = 628\text{nm}$ ,  $\theta_{\max} = 15\text{mas}$  and  $D = 2.4\text{m}$ . We obtain  $L_0 \approx \frac{\lambda}{\theta_{\max}} = 8.6\text{m}$  from Eq. (8). We compare Eqs.  $\Delta\theta$  with  $\Delta\theta_c$  in Fig. 5(a).

Similar to Sec. III, we consider the case without quantum memory. The total number of incident single photons to receivers is given by  $M_t = \sum_{k=0}^K \frac{2M}{\eta(2^{k-1}L_0)}$ . We compare our result ( $M_t$  and Eq. (10)) with  $\Delta\theta_c$  in Fig. 5(b). When  $\Delta\theta = 10^{-3}\text{mas}$ , we have  $K = 13$  then the length of fiber is  $2^{K-1}L_0 \approx 35\text{km}$  that is feasible for practical application.

## V. MORE GENERAL FORMULA

In Sec. II, we have shown how to detect the single-star target with the baseline  $L_k = 2^k L_0$ . It is easy to extend the method for more general case that  $L_{k+1} = s_k L_k$ , where integer  $s_k$  can take different value for different  $k$ .

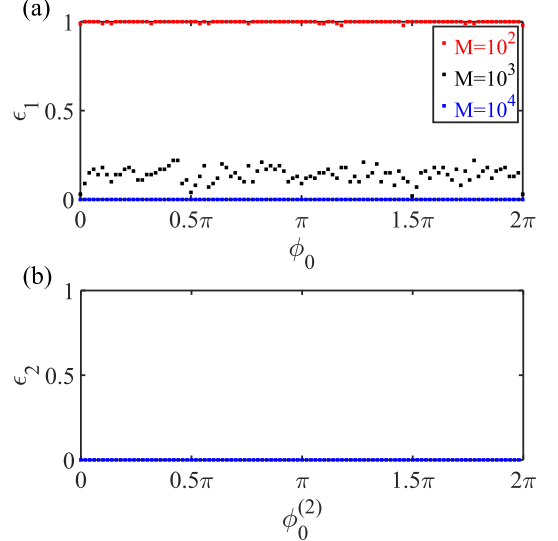


FIG. 4. The failure probability of distinguishing whether the target contains a single star or multiple stars. (a) The failure probability  $\epsilon_1$  of wrongly recognizing the single-star target as multiple stars.  $\phi_0$ : the phase of single star. We take  $M = 10^2$ ,  $10^3$  and  $10^4$ . (b) The failure probability of wrongly recognizing the two-star target as a single star. The phases of two stars are  $\phi_0^{(1)} = \pi$  and  $\phi_0^{(2)}$ . We take  $M = 10^4$ . Each data point is obtained by averaging 500 samples.

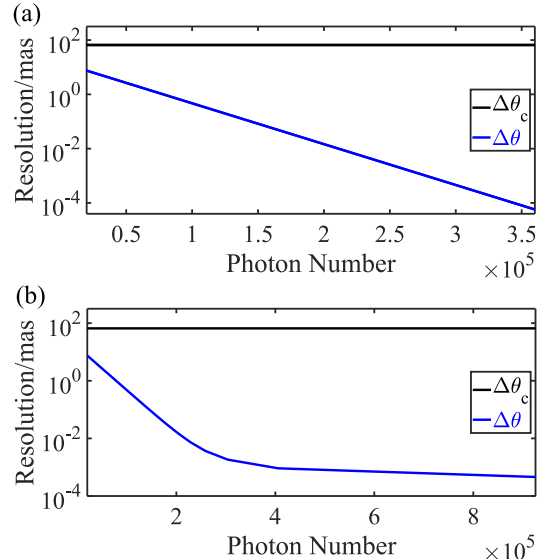


FIG. 5. Resolutions of Hubble Space Telescope  $\Delta\theta_c$  and our piecemeal quantum telescope  $\Delta\theta$  for general astronomical target. The horizontal axis is the total number  $M_t$  of incident single-photons to receivers. (a) Using quantum memory. (b) Not using quantum memory.

Directly, we have  $\phi_{k+1} = s_k \phi_k$ . Similar to Sec. II, we introduce a new variable

$$\psi_k = \phi_k - \hat{\phi}_k + \pi,$$

and its modulo

$$\dot{\psi}_k = (\phi_k - \hat{\phi}_k + \pi) \bmod 2\pi.$$

One can follow the similar proof of Sec. I in Supplementary Material [12], and obtain that the following equation

$$s_k \cdot \dot{\psi}_k = \dot{\psi}_{k+1} + \dot{r}_{k+1} + (s_k - 2)\pi. \quad (11)$$

can hold with a small failure probability if the observation error is not too large. Here  $r_{k+1} = \hat{\phi}_{k+1} - s_k \hat{\phi}_k + \pi$ . In particular, taking  $s_k = 2$  in Eq. (11) we obtain the formula in Eq. (2). Using Eq. (11) iteratively we have

$$\begin{aligned} \dot{\psi}_0 &= \prod_{r=0}^{K-1} \left( \frac{1}{s_r} \right) \left( \sum_{i=1}^{K-1} \prod_{j=i}^{K-1} s_j \dot{r}_i + \dot{r}_K + \dot{\psi}_K \right) \\ &\quad + \sum_{i=0}^{K-2} \prod_{j=i+1}^{K-1} (s_i - 2)s_j \pi + (s_{K-1} - 2)\pi \\ &= L_0 \left( \sum_{i=1}^K \frac{\dot{r}_i}{L_i} + \frac{\dot{\psi}_K}{L_K} + \sum_{i=0}^{K-1} \frac{(s_i - 2)\pi}{L_{i+1}} \right) \end{aligned} \quad (12)$$

where  $\prod_{j=0}^{i-1} s_j = L_i / L_0$  has been used. Recalling the definition  $\dot{\psi}_0 = (\phi_0 - \hat{\phi}_0 + \pi) \bmod 2\pi$  and taking the approximation  $\dot{\psi}_K = \pi$ , we obtain

$$\phi_0 = \left( \dot{\psi}_0 + \hat{\phi}_0 - \pi \right) \bmod 2\pi,$$

with  $\dot{\psi}_0$  given by Eq. (12).

## VI. CONCLUSION

We propose an efficient method of quantum telescope through bit-by-bit iteration. The super precision for our method requests only a small number of detected photons.

We acknowledge the financial support in part by National Natural Science Foundation of China grant No.11974204 and No.12174215, and Innovation Program for Quantum Science and Technology No. 2021ZD0300705. This study is also supported by the Taishan Scholars Program. We thank Prof. Y Cao of USTC for useful discussions.

- [3] Z. Huang, G. K. Brennen, and Y. Ouyang, Imaging stars with quantum error correction, *Physical Review Letters* **129**, 210502 (2022).
- [4] M. M. Marchese and P. Kok, Large baseline optical imaging assisted by single photons and linear quantum optics, *Physical Review Letters* **130**, 160801 (2023).
- [5] U. Zanforlin, C. Lupo, P. W. Connolly, P. Kok, G. S. Buller, and Z. Huang, Optical quantum super-resolution imaging and hypothesis testing, *Nature Communications* **13**, 5373 (2022).
- [6] L. Howard, G. Gillett, M. Pearce, R. Abrahao, T. Weinhold, P. Kok, and A. White, Optimal imaging of remote bodies using quantum detectors, *Physical review letters* **123**, 143604 (2019).
- [7] C. Lupo, Z. Huang, and P. Kok, Quantum limits to incoherent imaging are achieved by linear interferometry, *Physical Review Letters* **124**, 080503 (2020).
- [8] Z. Huang and C. Lupo, Quantum hypothesis testing for exoplanet detection, *Physical Review Letters* **127**, 130502 (2021).
- [9] Y. Wang, Y. Zhang, and V. O. Lorenz, Superresolution in interferometric imaging of strong thermal sources, *Physical Review A* **104**, 022613 (2021).
- [10] Z. Chen, A. Nomerotski, A. Slosar, P. Stankus, and S. Vintskevich, Astrometry in two-photon interferometry using an earth rotation fringe scan, *Physical Review D* **107**, 023015 (2023).
- [11] Z. Huang, C. Schwab, and C. Lupo, Ultimate limits of exoplanet spectroscopy: A quantum approach, *Physical Review A* **107**, 022409 (2023).
- [12] Supplementary material for ‘piecemeal quantum telescope with superresolution’.
- [13] Rayleigh, Xxi. investigations in optics, with special reference to the spectroscope, *The London, Edinburgh, and Dublin Philosophical Magazine and Journal of Science* **8**, 261 (1879).
- [14] M. Born and E. Wolf, *Principles of optics: electromagnetic theory of propagation, interference and diffraction of light* (Elsevier, 2013).
- [15] P. L. Chebyshev, Des valeurs moyennes, liouville’s, *J. Math. Pures Appl.* **12**, 177 (1867).
- [16] M. Loèv and M. Loèv, *Elementary probability theory* (Springer, 1977).

\* xbwang@mail.tsinghua.edu.cn

- [1] D. Gottesman, T. Jennewein, and S. Croke, Longer-baseline telescopes using quantum repeaters, *Physical review letters* **109**, 070503 (2012).
- [2] E. T. Khabiboulline, J. Borregaard, K. De Greve, and M. D. Lukin, Optical interferometry with quantum networks, *Physical review letters* **123**, 070504 (2019).

## Supplementary Material for ‘Piecemeal Quantum Telescope with Super Efficiency’

Sections I, II, III and IV are the supplement for main text of ‘Piecemeal Quantum Telescope with Super Efficiency’. In Sec. V, we introduce an alternative method for detecting single-star target whose failure probability is lower than the method in Sec. II of main text. In Sec. VI, we show a method for detecting the angle range of multiple-stars target.

### I. Mathematical derivation of iteration formula

Consider the formula below that relates the actual value  $\dot{\phi}_k$  and its observed value  $\hat{\phi}_k$

$$\hat{\phi}_k = (\dot{\phi}_k + e_k) \bmod 2\pi, \text{ for any } k,$$

where  $e_k \in (-\pi, \pi]$  can be regarded as the error of the observation.

Define  $r_{k+1} = \hat{\phi}_{k+1} - 2\hat{\phi}_k + \pi$ . For the equation

$$Z_k = 2 \cdot \dot{\psi}_k - \dot{\psi}_{k+1} - \dot{r}_{k+1},$$

consider the conditions:

$$\begin{cases} |e_k| < \pi, \\ |e_{k+1}| < \pi, \\ |e_{k+1} - 2e_k| < \pi. \end{cases}$$

Under these conditions, we demonstrate that  $Z_k = 0$ .

**Proof:** Observe the identity in modulo arithmetic:

$$(x \bmod 2\pi + y) \bmod 2\pi = (x + y) \bmod 2\pi.$$

Applying this identity, we derive the following:

$$\begin{aligned} 2 \cdot \dot{\psi}_k &= 2[(\dot{\phi}_k - (\dot{\phi}_k + e_k) \bmod 2\pi + \pi) \bmod 2\pi] \\ &= 2\pi - 2e_k, \\ \dot{\psi}_{k+1} &= (\dot{\phi}_{k+1} - (\dot{\phi}_{k+1} + e_{k+1}) \bmod 2\pi + \pi) \bmod 2\pi \\ &= \pi - e_{k+1}, \\ \dot{r}_{k+1} &= ((\dot{\phi}_{k+1} + e_{k+1}) \bmod 2\pi - 2(\dot{\phi}_k + e_k) \bmod 2\pi + \pi) \\ &\quad \bmod 2\pi \\ &= ((\dot{\phi}_{k+1} - 2(\dot{\phi}_k)) \bmod 2\pi + e_{k+1} - 2e_k + \pi) \bmod 2\pi. \end{aligned}$$

Given  $\dot{\phi}_{k+1} = (2 \cdot \dot{\phi}_k) \bmod 2\pi$ , it follows that:

$$(\dot{\phi}_{k+1} - 2 \cdot \dot{\phi}_k) \bmod 2\pi = 0.$$

Consequently,

$$\dot{r}_{k+1} = (e_{k+1} - 2e_k + \pi) \bmod 2\pi = e_{k+1} - 2e_k + \pi.$$

Hence,

$$\begin{aligned} Z_k &= 2 \cdot \dot{\psi}_k - \dot{\psi}_{k+1} - \dot{r}_{k+1} \\ &= 2\pi - 2e_k - (\pi - e_{k+1}) - (e_{k+1} - 2e_k + \pi) = 0. \quad \square \end{aligned}$$

From this we see that the event with  $Z_k \neq 0$  is very unlikely because it can only happens with large errors of observed values. Statistically, errors of observed values decrease rapidly with the rise of data size. Numerical simulation in Fig. 2 shows that a few detected photons can compress the failure probability to less than 1% for a high precision  $\frac{\pi}{2^{16}}$  of the result calculated by our Eq. (3).

### II. Collecting data with practical devices and weak incident light

Suppose the weak incident light contains a single photon with probability  $\varepsilon$  or vacuum with probability  $1 - \varepsilon$ . The state of incident light arriving at two receivers of pair  $k$  is  $\rho_k = (1 - \varepsilon)|\text{vac}\rangle\langle\text{vac}| + \varepsilon|\Psi_k\rangle\langle\Psi_k|$ , where

$$|\Psi_k\rangle = \frac{1}{\sqrt{2}}(|01\rangle + e^{i\phi_k}|10\rangle), \quad \phi_k \approx 2\pi \frac{L_k}{\lambda} \theta.$$

Suppose the detector has a dark count rate  $d$ , an imperfect detection efficiency  $\xi$ , and the channel has a transmittance  $\eta_k$ . After transmitting through the channel, the state becomes to

$$\rho'_k = (1 - \varepsilon')|\text{vac}\rangle\langle\text{vac}| + \varepsilon'|\Psi'_k\rangle\langle\Psi'_k|,$$

where  $\varepsilon' = \varepsilon\eta_k$ . After transmitting through the beam-splitter, the state is

$$\rho'_k = (1 - \varepsilon')|\text{vac}\rangle\langle\text{vac}| + \varepsilon'|\Psi'_k\rangle\langle\Psi'_k|,$$

where

$$|\Psi'_k\rangle = \frac{1}{2}(1 - e^{i\phi_k})|01\rangle + (1 + e^{i\phi_k})|10\rangle$$

Considering the dark count rate  $d$  and imperfect detection efficiency  $\xi$ , we obtain the probability of  $D_a$  silent and  $D_b$  clicking:

$$p_k = (1 - \varepsilon')(1 - d)d + \varepsilon'(1 - d)\xi \frac{1}{2}(1 - \cos \phi_k).$$

We detect totally  $M_k$  time-windows and observe the event of detector  $D_a$  silent and  $D_b$  clicking for  $m_k$  times. Taking the asymptotic approximation  $p_k \approx \frac{m_k}{M_k}$  we obtain

$$\cos \phi_k \approx 1 - 2 \frac{\frac{m_k}{M_k} - (1 - \varepsilon')(1 - d)d}{\varepsilon'(1 - d)\xi} := q_k. \quad (\text{S13})$$

Setting  $\frac{\pi}{2}$  phase shift for  $S$ , we observe the event of detector  $D_a$  silent and  $D_b$  clicking for  $\bar{m}_k$  times in total  $\bar{M}_k$  time-windows. Replacing  $\{m_k, M_k, \phi_k\}$  by  $\{\bar{m}_k, \bar{M}_k, \phi_k + \frac{\pi}{2}\}$  in Eq. (S13), we have

$$\sin \phi_k \approx 2 \frac{\frac{m_k}{M_k} - (1 - \varepsilon')(1 - d)d}{\varepsilon'(1 - d)\xi} - 1 := \bar{q}_k. \quad (\text{S14})$$

So we obtain  $\hat{\phi}_k = \frac{1}{2}(\cos^{-1} q_k + \sin^{-1} \bar{q}_k) \bmod 2\pi$ .

### III. Angular precisions of classical and existing quantum telescope

For a classical telescope with diameter  $D$ , the probability distribution of detected angle  $\theta_c$  is well-approximated by Gaussian function with the standard deviation  $\sigma(\theta_c) = \frac{\sqrt{2}\lambda}{\pi D}$  [3]. Taking Central-limit Theorem with 3 standard deviations and  $M_t$  incident photons, we formula the following precision of detected angle

$$\delta\theta_c := \frac{3\sigma(\theta_c)}{\sqrt{M_t}} = \frac{3\sqrt{2}\lambda}{\pi D\sqrt{M_t}}.$$

For a fair comparison, we assume the same initial crude information about angle  $\theta$  for existing quantum telescopes [1–4] and our method, i.e.,  $\theta \in [0, \theta_{\max}]$  and  $\theta_{\max}$  is a known value. Existing quantum telescopes with baseline  $l$  can detect the phase value in the range  $\phi \in [0, 2\pi)$  and the angle value in the range  $\theta \in [0, \lambda/l]$  [3]. Given the range above, the optimal length of baseline is  $l = \lambda/\theta_{\max}$ . Then the precision of existing quantum telescope is [3]:

$$\delta\theta_Q := \frac{3\sigma(\theta_Q)}{\sqrt{M_t}} \geq \frac{3\lambda}{2\pi l\sqrt{M_t}} = \frac{3\theta_{\max}}{2\pi\sqrt{M_t}},$$

where  $M_t$  is the incident photon number.

### IV. The proof of Theorem 1

Introduce the random variable  $X_k$ :

$$p\left(X_k = \sin\psi_k^{(n)}(\omega)\right) = p_n, \quad n = 1, 2, \dots, N,$$

where  $\psi_k^{(n)}(\omega) = \phi_k^{(n)} + \omega$ . The mean value  $\mu(X_k)$  and variance  $\sigma^2(X_k)$  are

$$\begin{aligned} \mu(X_k)_\omega &= \sum_n p_n \sin(\phi_k^{(n)} + \omega) = q_k \sin\omega + \bar{q}_k \cos\omega, \\ \mu(X_k^2)_\omega &= \sum_n p_n \sin^2(\phi_k^{(n)} + \omega) \\ &= \frac{1}{2} \left( 1 - \sum_n p_n \cos 2(\phi_k^{(n)} + \omega) \right) \\ &= \frac{1}{2} (1 - q_{k+1} \cos 2\omega + \bar{q}_{k+1} \sin 2\omega), \\ \sigma^2(X_k)_\omega &= \mu(X_k^2)_\omega - \mu(X_k)_\omega^2 = g_k(\omega). \end{aligned} \quad (\text{S16})$$

We see that  $g_k(\omega)$  is the variance of  $X_k$ . If  $N = 1$ ,  $X_k$  degenerates to a constant and its variance  $\sigma^2(X_k)_\omega$  vanishes for any  $\omega$ . So the function  $g_k(\omega)$  vanishes for any  $\omega$  including its maximal value  $g_k(\omega_k) = 0$ . The proof for necessary condition is completed. Now we prove the sufficiency.

The condition is that  $g_k(\omega_k)$  is the maximal value among all  $g_k(\omega)$  and  $g_k(\omega_k) = 0$ . It gives that  $\sigma^2(X_k)_{\omega_k}$

is the maximal value among all  $\sigma^2(X_k)_\omega$  and  $\sigma^2(X_k)_{\omega_k} = 0$ . Considering  $X_0$ , we conclude that  $\sin\psi_0^{(n)}(\omega_0)$  is the same for any  $n$ . It leads to two possible results:

- 1) All values in  $\{\psi_0^{(n)}(\omega_0)\}$  are the same, i.e.,  $N = 1$ ;
- 2)  $\exists x, y \in \{\psi_0^{(n)}(\omega_0)\}$ , s.t.,  $x + y = \pi$ .

Suppose  $\psi_0^{(1)}(\omega_0) + \psi_0^{(2)}(\omega_0) = \pi$  from case 2). We add an additional small phase  $\delta\omega$  and obtain

$$\begin{aligned} \sin\psi_0^{(1)}(\omega_0 + \delta\omega) &= \sin(\psi_0^{(1)}(\omega_0) + \delta\omega) \\ &= \sin(\pi - \psi_0^{(2)}(\omega_0) + \delta\omega) = \sin\psi_0^{(2)}(\omega_k - \delta\omega) \\ &\neq \sin\psi_0^{(2)}(\omega_k + \delta\omega). \end{aligned}$$

So  $\sigma^2(X_k)_{\omega_k + \delta\omega} > 0 = \sigma^2(X_k)_{\omega_k}$ . This counters the condition that  $\sigma^2(X_k)_{\omega_k}$  is the maximal value. So case 2) does not exist and we have  $N = 1$  from case 1).

### V. An alternative method for single-star target

We show an alternative method to determine the value of  $\phi_0$  by using the data  $\{q_k, \bar{q}_k | k = 0, 1, \dots, K\}$  from Eq. (5). We still set the baseline to be  $L_k = 2^k L_0$  and have  $\phi_{k+1} = 2\phi_k$ . We introduce the phase-slide function

$$\psi_k(\omega) = (\phi_k + \omega) \bmod 2\pi. \quad (\text{S17})$$

Applying Eqs. (S13) and (S14), we have

$$\sin\psi_k(\omega) \approx q_k \sin\omega + \bar{q}_k \cos\omega.$$

Maximizing  $\sin^2\psi_k(\omega)$  over  $\{\omega\}$ , we get two set of solutions

$$\begin{cases} \sin\omega_k = q_k, \cos\omega_k = \bar{q}_k, \\ \Rightarrow \omega_k = \frac{1}{2}(\sin^{-1}q_k + \cos^{-1}\bar{q}_k), \\ \sin\psi_k(\omega_k) \approx 1. \end{cases}$$

or

$$\begin{cases} \sin\omega_k = -q_k, \cos\omega_k = -\bar{q}_k, \\ \Rightarrow \omega_k = \frac{1}{2}(\sin^{-1}(-q_k) + \cos^{-1}(-\bar{q}_k)), \\ \sin\psi_k(\omega_k) \approx -1. \end{cases} \quad (\text{S18})$$

We choose anyone of these two solutions and define the binary value  $b_k$ : if  $\sin\psi_k(\omega_k) > 0 (< 0)$ , then  $b_k = 0 (\pi)$ .

*Theorem 2:* Asymptotically, given  $\omega_k$ ,  $b_k$ ,  $\omega_{k+1}$  and  $\psi_{k+1}(\omega_{k+1})$ , the value of  $\psi_k(\omega_k)$  is determined by the following form

$$\psi_k(\omega_k) = b_k + \frac{1}{2}[(\psi_{k+1}(\omega_{k+1}) + 2\omega_k - \omega_{k+1}) \bmod 2\pi].$$

*Proof:* We rewrite  $\psi_k(\omega_k)$  in the following form consisting of  $\psi_k(\omega_k) \bmod \pi$  and  $b_k := \psi_k(\omega_k) - \psi_k(\omega_k) \bmod \pi$

$\pi$

$$\begin{aligned}
& \psi_k(\omega_k) \\
&= b_k + \psi_k(\omega_k) \bmod \pi \\
&= b_k + (\phi_k + \omega_k + \frac{\omega_{k+1}}{2} - \frac{\omega_{k+1}}{2}) \bmod \pi \\
&= b_k + [(\phi_k + \frac{\omega_{k+1}}{2}) \bmod \pi + \omega_k - \frac{\omega_{k+1}}{2}] \bmod \pi \\
&= b_k + (\frac{(\phi_{k+1} + \omega_{k+1}) \bmod 2\pi}{2} + \omega_k - \frac{\omega_{k+1}}{2}) \bmod \pi \\
&= b_k + \frac{1}{2}[(\psi_{k+1} + 2\omega_k - \omega_{k+1}) \bmod 2\pi]. \quad (\text{S19})
\end{aligned}$$

Here  $\omega_{k+1}$  and  $\psi_{k+1}$  are obtained in the last iteration so only  $b_k$  is unknown and  $b_k = 0$  or  $\pi$ . From Eq. (S19) we also have if  $\sin \psi_k(\omega_k) > 0$  ( $< 0$ ), then  $b_k = 0$  ( $\pi$ ).  $\square$

*Method 2:* Given the detected data  $\{q_k, \bar{q}_k | k = 0, \dots, K\}$  in Eq. (5), we calculate  $\{\omega_k, b_k | k = 0, \dots, K\}$  from the content around Eq. (S18). Applying Theorem 2, we determine the value of  $\psi_k(\omega_k)$  iteratively

$$\psi_K(\omega_K) \Rightarrow \psi_{K-1}(\omega_{K-1}) \Rightarrow \dots \Rightarrow \psi_1(\omega_1) \Rightarrow \psi_0(\omega_0).$$

The initial condition is also given by Eq. (S18): if  $\sin \psi_K(\omega_K) \approx 1$  ( $-1$ ), then  $\psi_K(\omega_K) \approx \frac{1}{4}$  ( $\frac{3}{4}$ ). Applying Eq. (S17), we can get  $\phi_0$  from  $\psi_0(\omega_0)$

$$\phi_0 = (\psi_0(\omega_0) - \omega_0) \bmod 2\pi.$$

With the same precision as Eq. (6), we numerically simulate the failure probability of Method 2

$$\epsilon = P(|\tilde{\phi}_0 - \phi_0| > \frac{\pi}{2^{K+1}}).$$

where  $\tilde{\phi}_0$  is the result obtained from Method 2. Same to Sec. III in the main text, we calculate the failure probability with  $K = 14$ ,  $M = 1, 4$  and  $7$  as shown in Fig. (S6). We find that the failure probability in Fig. (S6) is lower than that in Fig. 2.

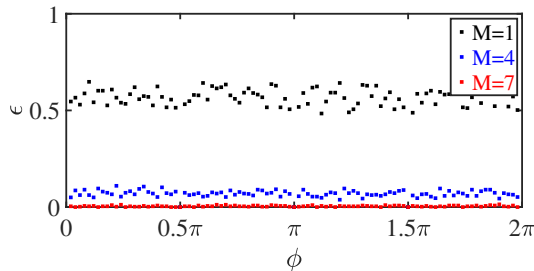


FIG. S6. The failure probability  $\epsilon$  changes with  $\phi$  for detecting single-star target by applying Method 2. We take  $M_k = \bar{M}_k = M$  for every  $k$ . The failure probability for the red data points is around 0.0046, about 63% of 0.0073 in Fig. 2. Each data point is obtained by averaging 500 samples.

## VI. Detecting the angle range of multiple-stars target

In Sec. IV of main text, we have shown how to distinguish whether the astronomical target contain a single star or multiple stars. If it is a single star, we can use the method in Sec. II of main text to detect its angle value. Here we show the method for detecting the angle range of multiple stars by using the data  $\{q_k, \bar{q}_k | k = 0, 1, \dots, K\}$  from Eq. (5). We still set the baseline to be  $L_k = 2^k L_0$  and have  $\phi_{k+1}^{(n)} = 2\phi_k^{(n)}$ . Introduce the phase-slide function

$$\psi_k^{(n)}(\omega) := (\phi_k^{(n)} + \omega) \bmod 2\pi, \quad (n = 1, 2, \dots, N), \quad (\text{S20})$$

and define

$$\begin{aligned}
f_k(\omega) &= q_k \sin \omega + \bar{q}_k \cos \omega, \\
g_k(\omega) &= \frac{1}{2} (1 - q_{k+1} \cos 2\omega + \bar{q}_{k+1} \sin 2\omega) - f_k(\omega)^2, \\
h_k(\omega) &= g_k(\omega) / f_k(\omega)^2,
\end{aligned}$$

for  $k = \{0, 1, \dots, K-1\}$ . Solving the equation  $h_k(\omega) \leq \bar{h}$  we obtain a range  $\omega \in \omega_k$  ( $\omega_k$  now denotes not a value, but a range). Define a binary function  $b_k(\omega)$ : if  $f_k(\omega) > 0$  ( $< 0$ ), then  $b_k(\omega) = 0$  ( $\pi$ ).

*Theorem 3:* Asymptotically, given a small  $\bar{h}$ ,  $\omega_k$ ,  $b_k(\omega)$ ,  $\omega_{k+1}$  and  $\{\psi_{k+1}^{(n)}(\omega) | n = 1, 2, \dots, N\}$ , with a small failure probability relating to  $\bar{h}$  we have

- 1) If  $\omega_k = \emptyset$ , then  $\psi_k^{(n)}(\omega) \in [0, 2\pi]$ .
- 2) If  $\omega_k \neq \emptyset$  and  $\omega_k \cap (\omega_{k+1}/2) = \emptyset$ , then  $\psi_k^{(n)}(\omega) \in b_k(\omega) + [0, \pi]$  over  $\omega \in \omega_k$ .
- 3) If  $\omega_k \neq \emptyset$  and  $\omega_k \cap (\omega_{k+1}/2) \neq \emptyset$ , then  $\psi_k^{(n)}(\omega) \in b_k(\omega) + \psi_{k+1}^{(n)}(2\omega)/2$  over  $\omega \in \omega_k \cap (\omega_{k+1}/2)$ .

To proof the Theorem 3, we first introduce the following lemma.

*Lemma for Theorem 3:* Asymptotically, given  $b_k(\omega)$ ,  $h_k(\omega)$ , and  $\{\psi_k^{(n)}(\omega) | n = 1, 2, \dots, N\}$ ,  $\exists \{\psi_k^{(m)}(\omega)\} \subseteq \{\psi_k^{(n)}(\omega)\}$ , s.t.

$$\psi_k^{(m)}(\omega) = b_k(\omega) + \frac{1}{2} \psi_{k+1}^{(m)}(2\omega),$$

with  $\sum_m p_m > 1 - h_k(\omega)$ .

*Proof:* As shown in Eq. (S16), our detected data does not directly give the information of  $\sin \psi_k^{(n)}(\omega)$ , but gives the mean value and variance of  $X_k$  whose possible value is  $\sin \psi_k^{(n)}(\omega)$ . *Chebyshev's inequality* [15, 16] gives that

$$p(|X_k - \mu(X_k)| \geq |\mu(X_k)|) \leq \frac{\sigma^2(X_k)}{\mu(X_k)^2} = \frac{g_k(\omega)}{f_k(\omega)^2} = h_k(\omega).$$

If the sign of  $X_k$  is different from the sign of  $\mu(X_k)$ ,  $|X_k - \mu(X_k)| > |\mu(X_k)|$  must hold. We get

$$p[\text{sgn}(X_k) \neq \text{sgn}(\mu(X_k))] < p(|X_k - \mu(X_k)| \geq |\mu(X_k)|) \leq h_k(\omega).$$

Applying the definition of  $X_k$ , we have

$$p[\operatorname{sgn}(X_k) = \operatorname{sgn}(\mu(X_k))] = \sum_m p_m$$

where  $\{\psi_k^{(m)}(\omega)\}$  satisfies  $\operatorname{sgn}(\sin \psi_k^{(m)}(\omega)) = \operatorname{sgn}(\mu(X_k))$ . So we obtain

$$\sum_m p_m > 1 - h_k(\omega).$$

Same to Eq. (S19), we rewrite  $\psi_k^{(m)}(\omega)$  as

$$\begin{aligned} \psi_k^{(m)}(\omega) &= b_k(\omega) + \psi_k^{(m)}(\omega) \bmod \pi \\ &= b_k(\omega) + (\phi_k^{(m)} + \omega) \bmod \pi \\ &= b_k(\omega) + \frac{1}{2}(\phi_{k+1}^{(m)} + 2\omega) \bmod 2\pi \\ &= b_k(\omega) + \frac{1}{2}\psi_k^{(m)}(2\omega). \end{aligned} \quad (\text{S21})$$

From Eq. (S21) we also have if  $\operatorname{sgn}(\sin \psi_k^{(m)}(\omega)) > 0 (< 0)$ , then  $b_k(\omega) = 0 (\pi)$ . Since  $\operatorname{sgn}(\sin \psi_k^{(m)}(\omega)) = \operatorname{sgn}(\mu(X_k)) = \operatorname{sgn}(f_k(\omega))$ , we have: if  $f_k(\omega) > 0 (< 0)$ , then  $b_k(\omega) = 0 (\pi)$ .  $\square$

*Proof of Theorem 3:* With a small failure probability relating to  $\bar{h}$ , for  $\omega \in \omega_k$  we obtain the approximation  $\sum_m p_m > 1 - h(\omega) \geq 1 - \bar{h} \approx 1$  and  $\{\psi_k^{(m)}(\omega)\} = \{\psi_k^{(n)}(\omega)\}$  in the Lemma, i.e.,

$$\psi_k^{(n)}(\omega) = b_k(\omega) + \frac{1}{2}\psi_{k+1}^{(n)}(2\omega), \quad n = \{1, 2, \dots, N\}. \quad (\text{S22})$$

1) If  $\omega_k = \emptyset$ , then Eq. (S22) is invalid since it does not have the domain of definition. We only have  $\psi_k^{(n)}(\omega) \in [0, 2\pi]$ .

2) If  $\omega_k \neq \emptyset$  and  $2\omega_k \cap \omega_{k+1} = \emptyset$ , then Eq. (S22) is valid over  $\omega_k$  but  $\psi_{k+1}^{(n)}(2\omega)$  is invalid over any subset of  $\omega_k$ . We have  $\psi_k^{(n)}(\omega) \in b_k(\omega) + [0, \pi)$  over  $\omega \in \omega_k$ .

3) If  $\omega_k \neq \emptyset$  and  $2\omega_k \cap \omega_{k+1} \neq \emptyset$ , then Eq. (S22) is valid over  $\omega_k$  and  $\psi_{k+1}^{(n)}(2\omega)$  is valid over  $2\omega_k \cap \omega_{k+1}$ . So we have  $\psi_k^{(n)}(\omega) \in b_k(\omega) + \frac{1}{2}\psi_{k+1}^{(n)}(2\omega)$  over  $\omega \in \omega_k \cap \omega_{k+1}$ .  $\square$

*Method 3:* Given the detected data  $\{q_k, \bar{q}_k | k = 0, 1, \dots, K\}$ , we calculate  $\{\omega_k, b_k(\omega) | k = 0, 1, \dots, K-1\}$  from the content below Eq. (S20). Applying the case 3) in Theorem 3, we determine the function in  $\{\psi_0^{(n)}(\omega) | n =$

$1, 2, \dots, N\}$  iteratively

$$\begin{aligned} &\left\{ \begin{array}{l} \psi_0^{(n)}(\omega) \in b_0(\omega) + \frac{\psi_1^{(n)}(2\omega)}{2}, \\ \omega \in \omega_0 \cap \frac{\omega_1}{2}, \end{array} \right. \Rightarrow \\ &\left\{ \begin{array}{l} \psi_0^{(n)}(\omega) \in b_0(\omega) + \frac{b_1(2\omega)}{2} + \frac{\psi_2^{(n)}(2^2\omega)}{2^2}, \\ \omega \in \omega_0 \cap \frac{\omega_1}{2} \cap \frac{\omega_2}{2^2}, \end{array} \right. \Rightarrow \\ &\dots \Rightarrow \\ &\left\{ \begin{array}{l} \psi_0^{(n)}(\omega) \in b_0(\omega) + \dots + \frac{b_{k-1}(2^{k-1}\omega)}{2^{k-1}} + \frac{\psi_k^{(n)}(2^k\omega)}{2^k}, \\ \omega \in \omega_0 \cap \dots \cap \frac{\omega_{k-1}}{2^{k-1}} \cap \frac{\omega_k}{2^k}, \end{array} \right. \end{aligned}$$

until we meet the case  $\omega_0 \cap \dots \cap \frac{\omega_k}{2^k} \cap \frac{\omega_{k+1}}{2^{k+1}} = \emptyset$ , then we terminate the iteration

$$\left\{ \begin{array}{l} \psi_0^{(n)}(\omega) \in b_0(\omega) + \dots + \frac{b_k(2^k\omega)}{2^k} + \frac{[0, \pi]}{2^k} \\ := [\psi_{\min}(\omega), \psi_{\max}(\omega)], \\ \omega \in \omega_0 \cap \dots \cap \frac{\omega_k}{2^k}. \end{array} \right. \quad (\text{S23})$$

So we obtain a range  $[\psi_{\min}(\omega), \psi_{\max}(\omega)]$  which includes all functions in  $\{\psi_0^{(n)}(\omega) | n = 1, 2, \dots, N\}$ . Applying Eq. (S20), we can get a range  $[\phi_{\min}, \phi_{\max}]$  which includes all values in  $\{\phi_0^{(n)} | n = 1, 2, \dots, N\}$ :  $\phi_{\min(\max)} = (\psi_{\min(\max)}(\omega) - \omega) \bmod 1$ . If  $\phi_{\min} < \phi_{\max}$ , the range is  $[\phi_{\min}, \phi_{\max}]$ ; else if  $\phi_{\min} > \phi_{\max}$ , the range is  $[\phi_{\min}, 2\pi) \cap [0, \phi_{\max}]$ . Without misunderstanding, we write in the unified form  $[\phi_{\min}, \phi_{\max}]$ . Remember  $\omega$  has a range given by Eq. (S23). So we take

$$\begin{aligned} \phi_{\min} &= \min_{\omega}[(\psi_{\min}(\omega) - \omega) \bmod 2\pi], \\ \phi_{\max} &= \max_{\omega}[(\psi_{\max}(\omega) - \omega) \bmod 2\pi]. \end{aligned}$$

The range  $[\phi_{\min}, \phi_{\max}]$  includes all values in  $\{\phi_0^{(n)}\}$  with a small failure probability relating to  $\bar{h}$ .

We show numerical simulation results of method 3. We detect a range which includes all phase values in  $\{\phi_0^{(n)}\}$ . We take all values in  $\{M_k, \bar{M}_k\}$  as the same value  $\frac{M}{s}$  and obtain a range  $[\phi_{\min}, \phi_{\max}]$ . Repeating the simulation for  $s$  times we get  $s$  values for  $\phi_{\min}$  and  $\phi_{\max}$ . Taking the average we obtain  $\langle \phi_{\min} \rangle$  and  $\langle \phi_{\max} \rangle$ . The failure probabilities is:

$$\begin{aligned} &\epsilon_3(\phi_0^{(1)}, \phi_0^{(2)}) \\ &= P(\phi_0^{(1)} \notin [\langle \phi_{\min} \rangle, \langle \phi_{\max} \rangle] \text{ or } \phi_0^{(2)} \notin [\langle \phi_{\min} \rangle, \langle \phi_{\max} \rangle]). \end{aligned}$$

We set  $M = 10^4$ ,  $\phi^{(1)} = \pi$ ,  $\phi^{(2)} \in (0, 2\pi)$ ,  $p_1 = p_2 = 0.5$ ,  $\bar{h} = 0.05$  and  $K = 13$ . The simulation results for  $\epsilon_3$  are shown in Fig. S7(a). We compare the real phase range  $|\phi_0^{(2)} - \phi_0^{(1)}|$  and the detected phase range  $(\langle \phi_{\max} \rangle - \langle \phi_{\min} \rangle) \bmod 2\pi$  in Fig. S7(b).

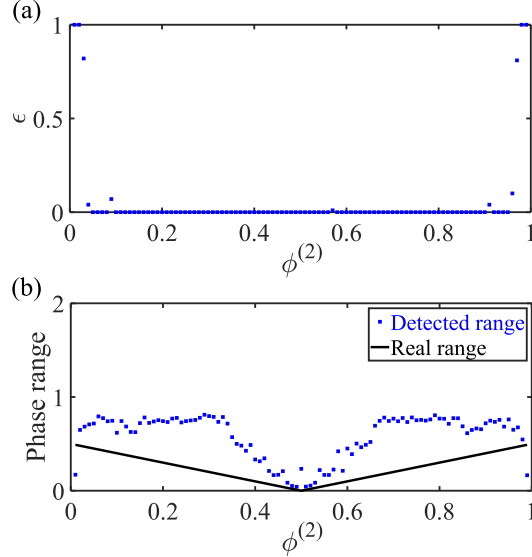


FIG. S7. (a) The failure probability  $\epsilon$  of estimating a phase range for two-star target. The phases of two stars are  $\phi_0^{(1)} = \pi$  and  $\phi_0^{(2)}$ . (b) Phase range of real value  $|\phi_0^{(2)} - \phi_0^{(1)}|$  and detected value  $(\langle \phi_{\max} \rangle - \langle \phi_{\min} \rangle) \bmod 2\pi$ .